

Actopaxin is phosphorylated during mitosis and is a substrate for cyclin B1/cdc2 kinase

Michael CURTIS, Sotiris N. NIKOLOPOULOS and Christopher E. TURNER¹

Department of Cell and Developmental Biology, State University of New York, Upstate Medical University, Syracuse, NY 13210, U.S.A.

Prior to cell division, normal adherent cells adopt a round morphology that is associated with a loss of actin stress fibres and disassembly of focal adhesions. In this study, we investigate the mitotic phosphorylation of the recently described paxillin and actin-binding focal-adhesion protein actopaxin [Nikolopoulos and Turner (2000) *J. Cell Biol.* **151**, 1435–1448]. Actopaxin is comprised of an N-terminus containing six putative cdc2 phosphorylation sites and a C-terminus consisting of tandem calponin homology domains. Here we show that the N-terminus of actopaxin is phosphorylated by cyclin B1/cdc2 kinase *in vitro* and that this region of actopaxin precipitates cdc2 kinase activity from mitotic lysates. Actopaxin exhibits reduced electrophoretic

mobility during mitosis that is dependent on phosphorylation within the first two consensus cdc2 phosphorylation sites. Finally, as cells progress from mitosis to G₁ there is an adhesion-independent dephosphorylation of actopaxin, suggesting that actopaxin dephosphorylation precedes cell spreading and the reformation of focal adhesions. Taken together, these results suggest a role for cyclin B1/cdc2-dependent phosphorylation of actopaxin in regulating actin cytoskeleton reorganization during cell division.

Key words: cell adhesion, cell cycle, parvin, phosphorylation.

INTRODUCTION

Cellular adhesion to the extracellular matrix (ECM) is essential for proliferation of non-transformed adherent cells. Adhesion to the ECM is mediated by integrins, a family of transmembrane glycoproteins that couple the ECM to the actin cytoskeleton [1]. The cytoplasmic tails of integrins interact with a variety of structural and signalling molecules, resulting in the recruitment of actin filaments and the formation of large complexes, termed focal adhesions [2,3].

Progression through the cell cycle involves periods of both robust and weak adhesion to the ECM. During mitosis, normal adherent cells frequently adopt a characteristic round morphology concomitant with dissolution of the actin cytoskeleton and disassembly of focal adhesions, resulting in a reduction in ECM adhesion. After cytokinesis, daughter cells re-establish contact with the ECM and stress fibres are reassembled. Additionally, attachment to the ECM is required to promote cyclin D1 and E1 expression, which are essential for G₁ phase progression [4–6].

Progression through the cell cycle is regulated by the cyclin-dependent kinases (Cdks or cdc2s), a family of serine/threonine kinases that are activated through an association with cyclin proteins [7,8]. The cyclin–cdc complex, cyclin B1/cdc2, mediates the transition into mitosis and is known to drive dramatic cellular changes, including nuclear envelope breakdown, spindle formation and chromosome condensation [9]. These changes are promoted through the phosphorylation of a variety of nuclear and cytoplasmic substrates, including histones, retinoblastoma protein and intermediate filament proteins [10–13]. The focal-adhesion proteins paxillin, focal-adhesion kinase (FAK), the Crk-associated substrate p130^{CAS} and zyxin have been demon-

strated to be phosphorylated during mitosis [14–16]. Mitotic phosphorylation of these focal-adhesion proteins may facilitate disassembly of focal adhesions and cell rounding prior to mitosis.

Recently, we described the identification and characterization of actopaxin, a focal-adhesion protein that associates with actin and paxillin [17]. In addition, we have shown that actopaxin interacts with integrin-linked kinase (ILK), a serine/threonine kinase that associates with the cytoplasmic tails of integrins [18,19]. Two actopaxin homologues, calponin homology (CH) domain-containing ILK-binding protein (CH-ILKBP) and afixin, have also been identified through their interaction with ILK [20,21]. The actopaxin C-terminus is comprised of tandem CH domains that are required for actin binding [22]. A paxillin-binding subdomain lies within the N-terminus of the second CH domain and mediates an association with the LD1 and LD4 motifs of paxillin [17,23]. Mutations in the paxillin-binding subdomain abrogate actopaxin focal-adhesion localization and result in retarded adhesion and cell spreading of HeLa cells plated on a collagen matrix [17]. The CH2 motif of actopaxin has also been shown to mediate an interaction with ILK [19–21]. The actopaxin N-terminus (amino acids 1–95) possesses no obvious secondary/tertiary structure but contains six potential cyclin B1/cdc2 kinase phosphorylation sites [24,25]. The cyclin B1/cdc2 complex is known to exhibit peak activity during mitosis and mediates the transition from the G₂ to the M phase [9]. In the present study we show that actopaxin is phosphorylated during mitosis. Mutational analysis identified the first two cdc2 consensus sites as targets for cyclin B1/cdc2 kinase activity. In addition, the N-terminus of actopaxin specifically precipitates cdc2 kinase activity. Finally, post-mitotic dephosphorylation of actopaxin occurs in an adhesion-independent fashion, suggesting that actopaxin dephosphorylation may be necessary for cell

Abbreviations used: ECM, extracellular matrix; ILK, integrin-linked kinase; CH, calponin homology; CH-ILKBP, CH domain-containing ILK-binding protein; GST, glutathione S-transferase; NP-40, Nonidet P-40; CIAP, calf intestinal alkaline phosphatase; 2D IEF, two-dimensional isoelectric focusing; CHO, Chinese hamster ovary; FAK, focal-adhesion kinase; SP, serine/proline.

¹ To whom correspondence should be addressed (e-mail turnerce@upstate.edu).

spreading and the reformation of focal adhesions following cytokinesis.

EXPERIMENTAL

DNA constructs and mutagenesis

Cloning of full-length actopaxin (amino acids 1–372), the N-terminal half (amino acids 1–222) and the C-terminal half (amino acids 222–372) as glutathione S-transferase (GST) fusion and Xpress-tagged constructs was described previously [17]. A GST fusion protein of the first 95 amino acids of actopaxin was generated by PCR amplification of amino acids 1–95 using PCR primers containing 5' *Bam*HI and 3' *Eco*RI restriction sites, followed by subcloning into a pGEX-2T vector (Pharmacia). Actopaxin point mutants S(4,8)G, S(14,19)G, S(4,8,14,19)G and S(4,8,14,19)G/S61A were generated using the QuikChange site-directed mutagenesis kit (Stratagene) according to the manufacturer's instructions. The sequence of all mutated constructs was verified by sequencing on both strands (BioResource Center, Cornell University, Ithaca, NY, U.S.A.).

Cell culture, synchronization and transfection

Chinese hamster ovary (CHO) K1 fibroblasts were cultured in modified Ham's F-12 medium (Mediatech) supplemented with 10% (v/v) fetal bovine serum (Atlanta Biologics), 2 mM glutamine, 50 units/ml penicillin and 50 µg/ml streptomycin (Sigma–Aldrich). HeLa and rat aortic smooth-muscle cells were cultured in Dulbecco's modified Eagle's medium (Mediatech) with the same supplements as Ham's F-12 medium. All cell lines were grown at 37 °C in a humidified chamber with 5% CO₂. Cells were arrested in mitosis by incubating with 8.3 nM nocodazole in the growth medium for 12–14 h. Cell populations enriched in cells at the G₂/M border were generated by incubating cells with 50 µM roscovitine (Calbiochem) in growth medium for 12 h.

HeLa cells were transfected using FuGene 6[™] (Roche) essentially as described by the manufacturer. Briefly, cells were plated at a density of 1 × 10⁶ cells/100 mm dish 14 h prior to transfection. FuGene 6[™] (8 µl) and 2 µg of the respective actopaxin construct were added to 200 µl of serum-free, antibiotic-free Dulbecco's modified Eagle's medium and incubated at 24 °C for 30 min. The lipid/DNA/media mixture was then added to the HeLa cells in complete Dulbecco's modified Eagle's medium. After transfection (14–16 h) cells were harvested using trypsin/EDTA and re-plated on fibronectin-coated plates. Transfected cells were arrested with nocodazole 3–5 h after re-plating to produce a transfected, mitotically arrested population.

Cell lysis

Adherent asynchronously growing cells were washed with PBS and lysed in 1% (v/v) Nonidet P-40 (NP-40) lysis buffer [10 mM Tris, pH 7.6, 50 mM NaCl, 1% NP-40, 10% (v/v) glycerol, 2 mM sodium pyrophosphate, 25 mM sodium β-glycerolphosphate, 25 mM NaF, 1 mM sodium orthovanadate, 1 mM *p*-nitrophenylphosphate, 5 mM benzamide and 10 µg/ml leupeptin] to produce the asynchronous lysates. Cells arrested in mitosis with nocodazole were collected by mechanical shake off from the culture plate, washed with 8.3 nM nocodazole in PBS and subsequently lysed in 1% NP-40 lysis buffer. Lysates were clarified by centrifugation and the soluble fraction collected in the supernatant. Protein concentrations of the soluble super-

natants were determined using the DC[™] protein assay (Bio-Rad) utilizing a BSA standard curve.

Preparation of fusion proteins

Escherichia coli (BL21) were transformed with GST–actopaxin constructs and grown for 14–16 h. Cultures were then diluted to a *D*₆₀₀ of 0.05 and grown until the *D*₆₀₀ value reached 0.5–0.8, when protein expression was induced by the addition of 1 mM isopropyl β-D-thiogalactoside. Fusion proteins were then harvested and purified as described previously [26].

In vitro GST pull-down and cyclin B1/cdc2 kinase assays

For cyclin B1/cdc2 kinase assays, cyclin B1/cdc2 complexes were immunoprecipitated out of lysates from asynchronous and mitotically arrested CHO.K1 cells using a cyclin B1 monoclonal antibody (Santa Cruz Laboratories). Soluble supernatants were prepared using 1% NP-40 lysis buffer. Immunoprecipitated cyclin B1/cdc2 complexes were washed with 1% NP-40 lysis buffer and then in kinase buffer (50 mM Hepes, pH 7.5, 10 mM MnCl₂, 10 mM MgCl₂, 2 mM sodium pyrophosphate, 25 mM sodium β-glycerolphosphate, 25 mM NaF, 1 mM sodium orthovanadate and 1 mM *p*-nitrophenylphosphate). The substrate GST fusion proteins were eluted from GSH–agarose and dialysed into kinase buffer. Cyclin B1/cdc2 complexes were incubated with approx. 10 µg of the respective GST fusion protein, in a final volume of 50 µl containing 10 µCi of [³²P]ATP. Incubation was carried out at 24 °C for 30 min.

For pull-down assays, approx. 30 µg of GST fusion protein was immobilized on GSH–agarose beads and equilibrated in 1% NP-40 lysis buffer. Asynchronous and mitotically arrested cells were lysed in 1% NP-40 buffer and aliquots (100 µg, approx. 0.5 mg/ml) were incubated with the respective fusion proteins for 3 h at 4 °C. The GSH–agarose beads were washed with 1% NP-40 lysis buffer and then with kinase buffer. Kinase reactions were conducted at 24 °C for 30 min in a final volume of 50 µl containing GSH–agarose beads, 10 µCi of [³²P]ATP and 10 µg of histone H1.

All kinase reactions were stopped by boiling in Laemmli sample buffer. Samples were resolved by SDS/PAGE (12.5% gels), stained with Coomassie Brilliant Blue and visualized by autoradiography.

Phosphopeptide mapping and phospho amino acid analysis

Phosphorylated proteins from the *in vitro* kinase assays were excised from dried SDS/PAGE gels, rehydrated with water and macerated using a microtube pestle. The gel pieces were dehydrated with 50% methanol/50% water and then dried completely in a vacuum concentrator. Dried gel pieces were re-swollen in 50 mM ammonium bicarbonate, pH 8.3, with 0.2 mg/ml trypsin and incubated at 37 °C for 16 h. Tryptic peptides were then extracted using 50% methanol/1.3% formic acid/3.9% glacial acetic acid/44.8% water. The extract was concentrated in a vacuum concentrator and reconstituted in TLE buffer, pH 1.9 (2.5% formic acid/7.8% glacial acetic acid/89.7% water). Phosphopeptides were analysed by a standard two-dimensional phosphopeptide mapping technique [27]. Phosphopeptides were separated in the first dimension by thin-layer electrophoresis at pH 1.9 and then resolved further by TLC using a mobile phase of 37.5% *n*-butanol/25% pyridine/7.5% glacial acetic acid/30% water. Aliquots of the tryptic peptides were

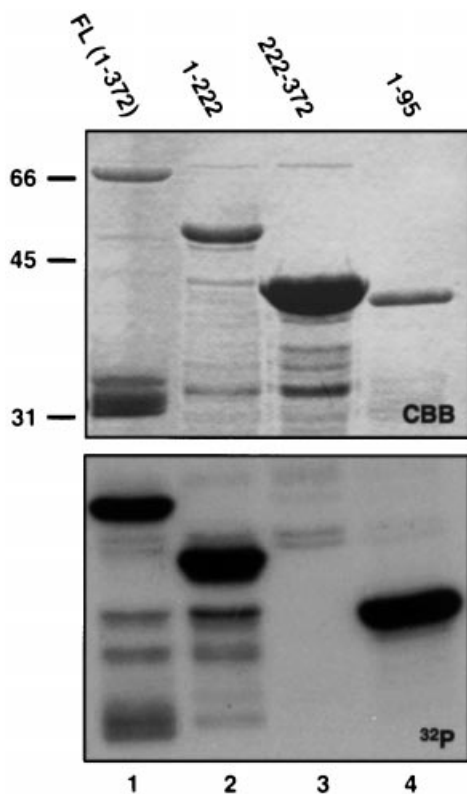


Figure 2 Cyclin B1/cdc2 kinase phosphorylates actopaxin *in vitro*

Cyclin B1/cdc2 *in vitro* kinase assays using cyclin B1/cdc2 complexes isolated from cells arrested in mitosis with nocodazole. Immunoprecipitated cyclin B1/cdc2 complexes were incubated with approx. 10 μ g of the following GST fusion proteins: full-length GST-actopaxin [FL(1–372)], GST-actopaxin amino acids 1–222 (1–222), GST-actopaxin amino acids 222–372 (222–372) and GST-actopaxin amino acids 1–95 (1–95). The upper panel shows the Coomassie Brilliant Blue (CBB) stain of the kinase reactions analysed by SDS/PAGE, and the lower panel shows the corresponding autoradiograph (32 P). The phosphorylation of actopaxin is localized to the first 95 amino acids.

incubated with active cyclin B1/cdc2 complexes immunoprecipitated from mitotic CHO.K1 fibroblasts followed by kinase assays [29]. Cyclin B1/cdc2 is able to phosphorylate full-length actopaxin, and amino acids 1–222 and 1–95 (Figure 2, lanes 1, 2 and 4). However, cyclin B1/cdc2 did not phosphorylate the C-terminus of actopaxin (Figure 2, lane 3).

Phosphoamino acid analysis of actopaxin and the N-terminus of actopaxin (amino acids 1–95), phosphorylated by cyclin B1/cdc2 kinase, showed predominantly serine phosphorylation (Figure 3B, lanes 1 and 2). Phosphopeptide mapping of full-length actopaxin produced two spots, A and B (Figure 3C, panel 1). Phosphoamino acid analysis of these two spots showed that they both contained phosphoserine (results not shown).

To begin to delineate which residues of actopaxin are involved in cyclin B1/cdc2-dependent phosphorylation, a series of serine point mutants were generated. The effect of mutations on cyclin B1/cdc2 kinase phosphorylation was tested using GST-actopaxin fusion proteins incubated with precipitated cyclin B1/cdc2 kinase, which were then subjected to *in vitro* kinase assays. Mutation of Ser-4 and Ser-8 to glycine [S(4,8)G] had no apparent effect on the net phosphorylation of actopaxin (Figure 3A, lane 6, and Figure 3B, lane 3). Phosphopeptide mapping, however, showed that the lower of the two spots, spot B, observed with

wild-type actopaxin, had been eliminated (Figure 3C, panel 2), indicating that the peptide corresponding to spot B contained Ser-4 and Ser-8. Mutation of Ser-14 and Ser-19 to glycine [(S(14,19)G)] also had little effect on the overall phosphorylation of actopaxin (Figure 3A, lane 7, and Figure 3B, lane 4). However in this instance, the phosphopeptide map showed that the upper of the two spots, spot A, observed with wild-type actopaxin was missing (Figure 3C, panel 3). These data are consistent with spot A containing Ser-14 and Ser-19. Spots C and D, observed in the phosphopeptide maps of the S(4,8)G and S(14,19)G mutants respectively, are not observed in wild-type actopaxin phosphopeptide maps and may represent artifacts resulting from the mutagenesis (see below). To verify the spot assignments, phosphopeptide-mixing experiments were performed using wild-type actopaxin and the two serine double point mutants S(4,8)G and S(14,19)G (results not shown), as well as a mixture of the two serine double point mutants (Figure 3C, panel 4). All three mixtures gave the wild-type two-spot pattern, confirming the assignments of spot A and B. Mutation of the fifth SP site, Ser-61, had no effect on the phosphorylation of actopaxin by cyclin B1/cdc2 kinase *in vitro* and produced a phosphopeptide map that was identical to the wild-type phosphopeptide profile (results not shown).

To characterize the cyclin B1/cdc2 phosphorylation profile of actopaxin further, quadruple [S(4,8,14,19)G] and pentad [S(4,8,14,19)G/S61A] mutants were generated and evaluated in the GST-actopaxin fusion protein/cyclin B1/cdc2 *in vitro* kinase assay. Both mutants demonstrated a significant reduction in the phosphorylation of actopaxin by cyclin B1/cdc2 kinase (Figure 3A, lanes 9 and 10). Interestingly, these mutants showed predominantly threonine phosphorylation (Figure 3B, lanes 6 and 7). Phosphopeptide map analysis of the quadruple SP mutant showed the loss of both spot A and B and the appearance of two unique spots, spots E and F (Figure 3C, panel 5). These new spots were confirmed to be different from A and B by mixing with phosphopeptides from wild-type actopaxin (Figure 3C, panel 6). Phosphoamino acid analysis showed that spots E and F contained phosphothreonine (results not shown). The threonine phosphorylation is likely to be an artifact of the mutagenesis since wild-type actopaxin is phosphorylated only on serine in this assay (Figure 3B, lane 1) and spots E and F are not observed in wild-type actopaxin (Figure 3C, panel 1). Mutating the serine phosphorylation sites may allow Thr-16 to become accessible for phosphorylation. Taken together these data indicate that a combination of sites 4, 8, 14 and 19 can be phosphorylated *in vitro* by cyclin B1/cdc2.

The N-terminus of actopaxin precipitates cyclin B1/cdc2 kinase activity

We next tested whether actopaxin could directly precipitate and be phosphorylated by cyclin B1/cdc2 kinase. To address this, GST pull-down kinase assays were performed using lysates from asynchronous and mitotic cells (see the Experimental section). Histone H1 was added as an exogenous substrate. GST-actopaxin and histone H1 were phosphorylated by the kinase activity precipitated from mitotic lysates with GST-actopaxin (Figure 4A, lane 4). Kinase activity was absent in pull-down assays performed with asynchronous lysates (Figure 4A, lane 3). The N-terminal half of actopaxin (amino acids 1–222) also specifically precipitated kinase activity from mitotic lysates (Figure 4A, lanes 5 and 6). In addition, a GST-fusion protein consisting of the first 95 amino acids of actopaxin was sufficient to precipitate kinase activity from mitotic lysates (Figure 4B, lane 1 and 2). Kinase activity was not detected in pull-down assays performed

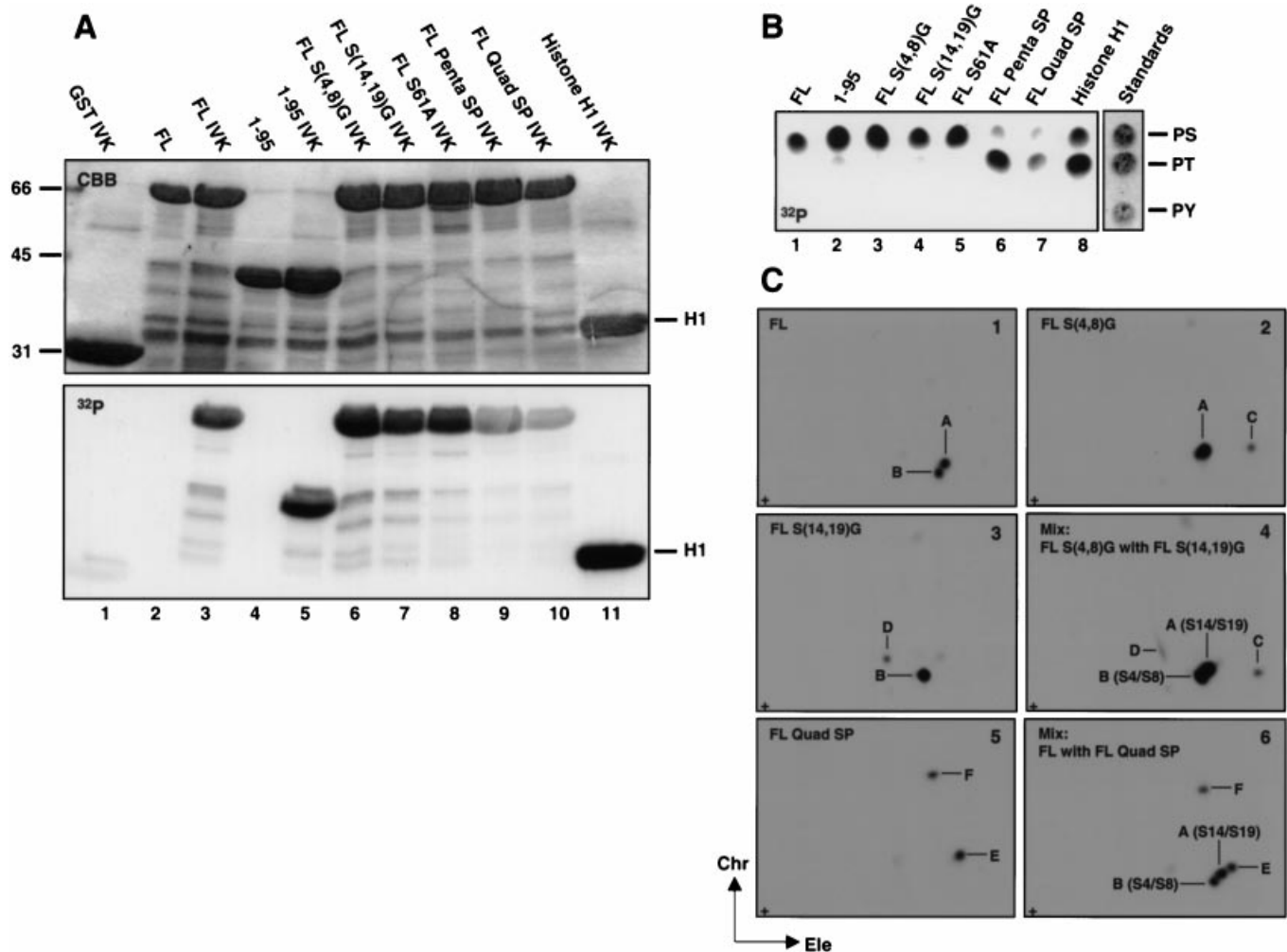


Figure 3 Cyclin B1/cdc2 kinase phosphorylates actopaxin within the first four SP sites

(A) Cyclin B1/cdc2 *in vitro* kinase assays (IVKs) using GST–actopaxin phospho-mutants. Cyclin B1/cdc2 complexes were immunoprecipitated from mitotic whole-cell lysates and were incubated with approx. 30 μ g of the following GST–actopaxin fusion proteins: GST, full-length GST–actopaxin (FL), GST–actopaxin amino acids 1–95 (1–95), GST–actopaxin S(4,8)G double point mutant [FL S(4,8)G], GST–actopaxin S(14,19)G double point mutant [FL S(14,19)G], GST–actopaxin S61A single point mutant (FL S61A), GST–actopaxin S(4,8,14,19)G/S61A penta point mutant (FL Penta SP) and GST–actopaxin S(4,8,14,19)G quadruple point mutant (FL Quad SP). H1, histone H1. The upper panel shows the Coomassie Brilliant Blue (CBB) stain of the kinase reactions analysed by SDS/PAGE, and the lower panel shows the corresponding autoradiograph (32 P). Only when the first four SP sites were mutated was there a significant reduction in the *in vitro* phosphorylation of actopaxin by cyclin B1/cdc2 kinase. (B) Phosphoamino acid analysis of proteins phosphorylated in cyclin B1/cdc2 *in vitro* kinase assays. Ninhydrin-stained phosphoamino acid standards are shown on the right. PS, phosphoserine; PT, phosphothreonine; PY, phosphotyrosine. Actopaxin is phosphorylated on serine by cyclin B1/cdc2 kinase. The Quad and Penta SP mutants showed a loss of serine phosphorylation and an increase in threonine phosphorylation. (C) Phosphopeptide mapping of proteins phosphorylated in cyclin B1/cdc2 *in vitro* kinase assays. Ele, electrophoresis dimension; Chr, chromatographic dimension; + indicates the origin. Phosphopeptides corresponding to phosphorylation sites S4/S8 and S14/S19 are labelled B and A respectively. See the Results section for discussion of peptides C–F.

using the C-terminal half of actopaxin (Figure 4A, lanes 7 and 8) or GST alone (Figure 4A, lanes 1 and 2). These data demonstrate that the N-terminus of actopaxin is capable of precipitating mitosis-specific kinase activity.

Phosphoamino acid analysis of histone H1 from the full-length GST–actopaxin pull-down kinase assay yielded phosphoserine and phosphothreonine, whereas analysis of GST–actopaxin and GST–actopaxin (1–95) yielded predominantly phosphoserine (Figure 4C, lanes 1, 2 and 3 respectively). Phosphopeptide maps were generated for GST–actopaxin, GST–actopaxin (1–95) and histone H1 (Figure 4D, panels 1, 3 and 5). These maps were compared with the phosphopeptide maps of the same proteins phosphorylated in the cyclin B1/cdc2 *in vitro* kinase assays described above (Figure 4D, panels 2, 4

and 6). The phosphopeptide maps for GST–actopaxin yielded identical patterns consisting of two spots (spots A and B; Figure 4D, panels 1 and 2). GST–actopaxin (1–95) phosphopeptide maps from both kinase assays are also identical; however, the migration of the lower of the two spots differs from full-length wild-type actopaxin (labelled as B*; Figure 4D, panels 3 and 4). This difference has been confirmed in mixing experiments (results not shown). Tryptic digests of this portion of actopaxin may result in alternative fragmentation relative to digests of the full-length protein, resulting in the generation of different phosphopeptides. Spot B* may also result from phosphorylation at alternative sites within the 1–95 segment of actopaxin. The phosphopeptide maps of histone H1 from the GST–actopaxin pull-down and cyclin B1/cdc2 kinase assays were also identical (Figure 4D, panels 5

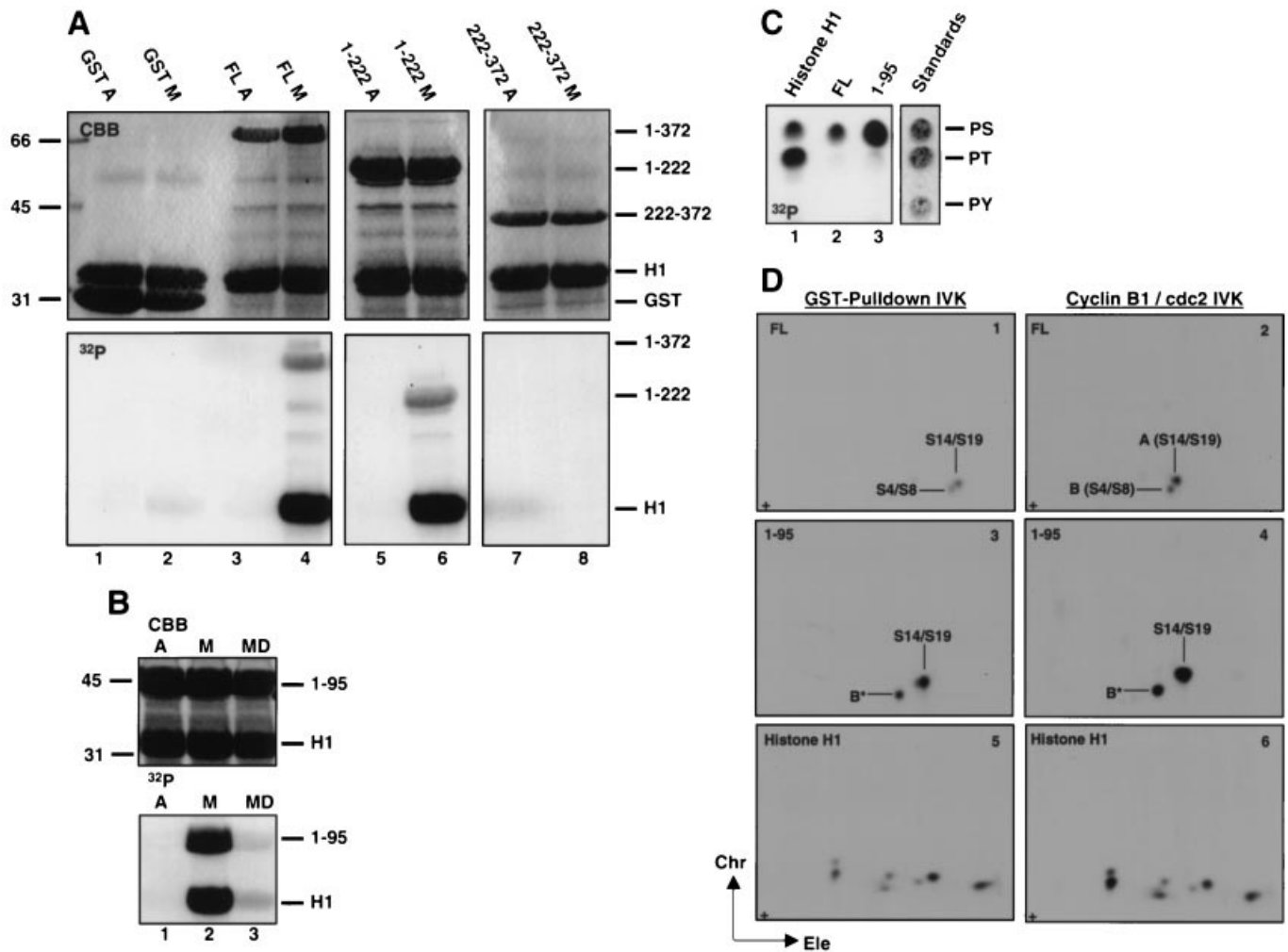


Figure 4 Actopaxin precipitates cyclin B1/cdc2 kinase activity

(A) GST pull-down kinase assays using GST, GST-actopaxin (FL), GST-actopaxin amino acids 1-222 (1-222) and GST-actopaxin amino acids 222-372 (222-372), bound to GSH-agarose beads. Pull-downs were done from an adherent asynchronous population (A) and cells mitotically arrested with nocodazole (M). Histone H1 (H1) was added to each kinase reaction. The upper panels show the Coomassie Brilliant Blue (CBB) stain of the kinase reactions analysed by SDS/PAGE, and the lower panels show the corresponding autoradiograph (³²P). Only full-length actopaxin and actopaxin 1-222 were able to precipitate kinase activity that could phosphorylate the GST fusion protein and histone H1. The kinase activity was only precipitated from mitotic lysates. (B) GST pull-down kinase assays using amino acids 1-95 of actopaxin. Pull-downs were done from an adherent asynchronous population (A), cells mitotically arrested with nocodazole (M), and a mitotic cell lysate that was immunodepleted of cyclin B1/cdc2 complexes (MD). A significant reduction in the kinase activity precipitated by actopaxin 1-95 was observed when the mitotic lysate was depleted of cyclin B1/cdc2 complexes. (C) Phosphoamino acid analysis of proteins phosphorylated in GST pull-down kinase assays. Ninhydrin-stained phosphoamino acid standards are shown on the right. PS, phosphoserine; PT, phosphothreonine; PY, phosphotyrosine. The kinase activity precipitated by FL actopaxin and actopaxin 1-95 phosphorylated both proteins on serine and histone H1 on serine and threonine. (D) Phosphopeptide mapping of proteins phosphorylated in GST pull-down kinase assays. Ele, electrophoretic dimension; Chr, chromatographic dimension; + indicates the origin. Phosphopeptide maps generated from proteins phosphorylated in the GST pull-down kinase assays were identical to those generated from the same proteins phosphorylated by immunoprecipitated cyclin B1/cdc2 kinase. IVK, *in vitro* kinase assay.

and 6). The similarity in the phosphopeptide maps from the GST pull-down and cyclin B1/cdc2 *in vitro* kinase assays of both actopaxin and histone H1 suggests that the kinase activity precipitated in the GST pull-down kinase assays was the result of cyclin B1/cdc2 kinase activity physically associated with the N-terminus of actopaxin.

To demonstrate that the kinase activity being precipitated in the GST pull-down kinase assays was cdc2 kinase, an immunodepletion experiment was conducted since Western blotting of the precipitates proved inconclusive. Mitotic lysates were immunodepleted of cyclin B1/cdc2 complexes by immunoprecipitation with cyclin B1 monoclonal antibodies. To confirm adequate depletion, the depleted lysate was re-immunoprecipitated with

cyclin B1 and the immunoprecipitate was tested for kinase activity against histone H1. The immunoprecipitate from the sequential immunoprecipitation did not show kinase activity towards histone H1, confirming depletion (results not shown). The mitotic, immunodepleted lysate (MD) was then used in a GST pull-down kinase assays with actopaxin (1-95). In contrast with precipitation from the complete mitotic lysate, GST-actopaxin (1-95) was unable to precipitate any kinase activity from the depleted lysate, as measured by the lack of phosphorylation of either actopaxin (1-95) or exogenously added histone H1 (Figure 4B, lane 3). These data, taken together with the phosphopeptide map analysis, supports the conclusion that cyclin B1/cdc2 kinase activity was precipitated by actopaxin,

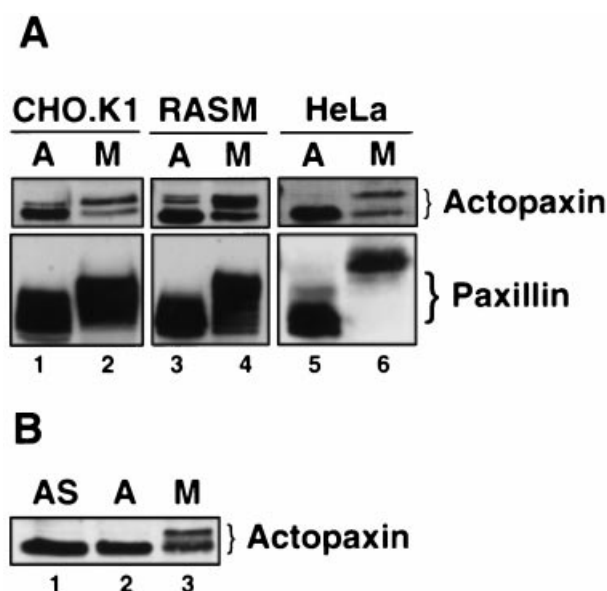


Figure 5 Actopaxin displays reduced electrophoretic mobility in mitosis

(A) Western-blot analysis of whole-cell lysates (50 μ g total protein) from CHO.K1 fibroblasts, rat aortic smooth-muscle cells (RASM) and human cervical carcinoma (HeLa) cells probed with anti-actopaxin polyclonal antiserum. A, an adherent asynchronous population; M, cells mitotically arrested with nocodazole. The blot was reprobed with an anti-paxillin monoclonal antibody. Both actopaxin and paxillin showed reduced electrophoretic mobility in the mitotic lysates. (B) Western-blot analysis of CHO.K1 whole-cell lysates probed with anti-actopaxin polyclonal antiserum. AS, cells growing asynchronously in suspension. The reduced electrophoretic mobility of actopaxin was only observed in the mitotic lysate.

and that the cyclin B1/cdc2 phosphorylation and binding sites reside in the first 95 amino acids of actopaxin.

Actopaxin is phosphorylated during mitosis

Protein phosphorylation is often accompanied by a reduction in the electrophoretic mobility of the protein when compared with its non-phosphorylated form. To determine whether actopaxin was phosphorylated *in vivo* during mitosis, we prepared asynchronous and mitotic lysates from CHO.K1 fibroblasts, rat aortic smooth-muscle cells and human cervical carcinoma cells (HeLa), and probed them with anti-actopaxin antiserum. A slower-migrating form of actopaxin was clearly observed in all mitotic lysates (Figure 5A, lanes 2, 4 and 6). Paxillin, which also demonstrates a mitosis-specific electrophoretic mobility shift, was used as a positive control for these experiments [14,15]. The shifted form of actopaxin is reduced substantially or absent in lysates from asynchronously growing cells (Figure 5A, lanes 1, 3 and 5). Additionally, the slower-migrating form is absent from asynchronously growing cells that have been held in suspension following EDTA release from the culture dish, indicating that the actopaxin mobility shift is mitosis-specific and not simply a result of loss of adhesion to the ECM (Figure 5B).

To confirm that the reduced electrophoretic mobility of actopaxin was due to phosphorylation, we analysed whole-cell lysates by 2D IEF/SDS/PAGE and also evaluated the effect of alkaline phosphatase treatment. In 2D IEF/SDS/PAGE analysis, phosphorylated proteins exhibit an acidic shift relative to their non-phosphorylated form [28,30]. Whole-cell lysates from asynchronous and mitotic CHO.K1 fibroblasts were focused in a

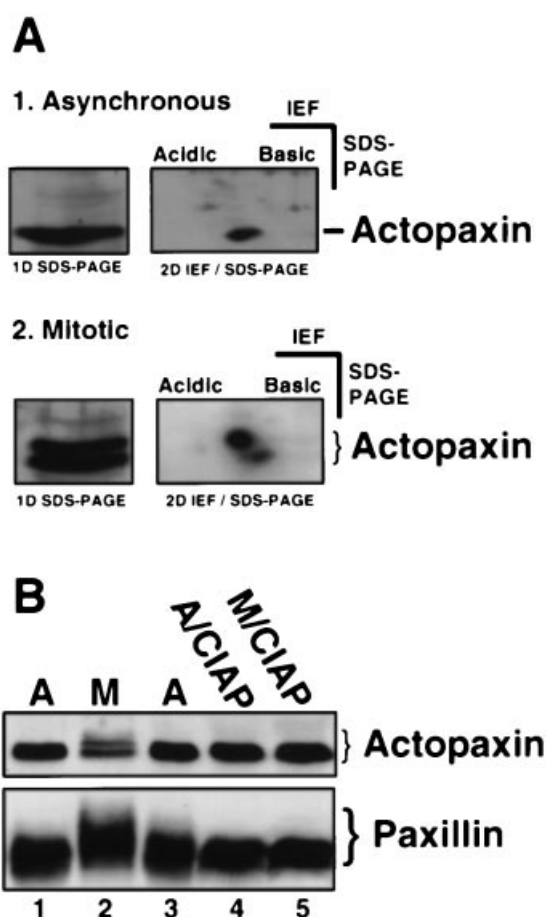


Figure 6 Reduced electrophoretic mobility of actopaxin during mitosis is due to phosphorylation

(A) 2D IEF-SDS/PAGE followed by Western-blot analysis of whole-cell lysates (50 μ g total protein) from asynchronously growing and mitotically arrested CHO.K1 fibroblasts probed with anti-actopaxin polyclonal antibody. Note the acidic shift in the reduced mobility form of actopaxin. (B) Western-blot analysis of CHO.K1 whole-cell lysates (50 μ g total protein) treated with alkaline phosphatase and probed with anti-actopaxin polyclonal antibody. The blot was reprobed with anti-paxillin monoclonal antibody. The mobility shift of actopaxin and paxillin was lost upon CIAP treatment. A and M are defined in the Figure 5 legend.

pH gradient of 3–10, resolved on a 12.5% acrylamide slab gel and then immunoblotted for actopaxin (Figure 6A). The asynchronous lysate demonstrated one band in the one-dimensional SDS/PAGE analysis and one major spot when subjected to 2D IEF/SDS/PAGE analysis (Figure 6A, upper panels). In contrast, the mitotic lysate exhibited two bands in the one-dimensional SDS/PAGE analysis and two-major spots in the 2D IEF/SDS/PAGE (Figure 6A, bottom panels). The higher-molecular-mass spot in the 2D IEF/SDS/PAGE immunoblot demonstrated an acidic shift relative to the lower-molecular-mass spot and corresponded to the higher-molecular-mass band in the one-dimensional SDS/PAGE immunoblot. This acidic shift suggests that the form of actopaxin exhibiting reduced mobility was phosphorylated. To confirm this, whole-cell lysates from asynchronous and mitotic CHO.K1 fibroblasts were prepared in the absence of phosphatase inhibitors, treated with CIAP and analysed by Western blotting (Figure 6B). Treatment of the mitotic lysates with CIAP eliminated the reduced mobility form

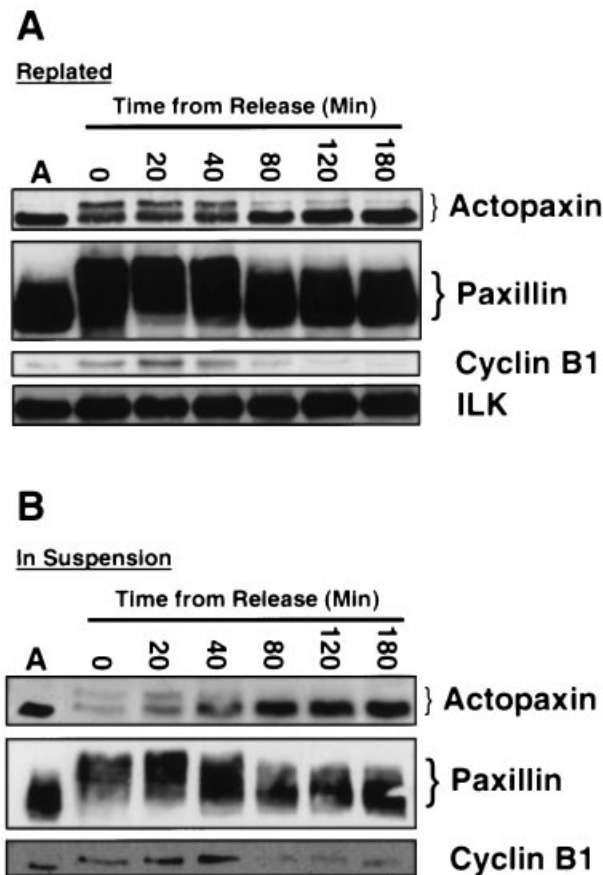


Figure 7 Dephosphorylation of actopaxin is adhesion-independent

(A) CHO.K1 fibroblasts were arrested with nocodazole, collected and subsequently released from mitotic arrest by washing out the nocodazole and re-plating (lane A). Whole-cell lysates were collected at the indicated time points after release and analysed by Western-blot analysis (50 μ g total protein). The blot was probed with anti-actopaxin polyclonal antiserum and anti-paxillin, anti-(cyclin B1) and anti-ILK monoclonal antibodies. Actopaxin and paxillin both show a reversal of their mobility shifts between 40 and 80 min. Cyclin B1 reprobe was included to demonstrate the transition out of mitosis. (B) Cells were arrested and released as described above and were subsequently put into suspension. Whole-cell lysates were collected at the indicated time points after release and analysed by Western-blot analysis (25 μ g total protein). The blot was probed with anti-actopaxin polyclonal antiserum, and anti-paxillin and anti-(cyclin B1) monoclonal antibodies. The reversal of actopaxin and paxillin mobility shifts was similar to that observed when the cells were allowed to adhere.

of both actopaxin and paxillin. These data confirm that actopaxin undergoes mitosis-dependent phosphorylation.

Reversal of the actopaxin mitotic mobility shift is adhesion-independent

The phosphorylation of actopaxin coincided with cell rounding prior to mitosis. We next investigated the dependence of actopaxin dephosphorylation on the establishment of new cell-ECM adhesions following mitosis/cell division. CHO.K1 fibroblasts, arrested in mitosis, were harvested and released from the nocodazole block to allow exit from M phase and entry into G_1 . One population of cells was released on to a tissue-culture dish and allowed to adhere, while a second population was maintained in suspension following nocodazole washout. Whole-cell lysates were prepared at specific time intervals and the lysates were analysed by immunoblotting (Figure 7). The mobility shift of

actopaxin was lost between 40 and 80 min, in both the re-plated (Figure 7A) and suspended (Figure 7B) populations, indicating that the dephosphorylation of actopaxin is adhesion-independent. The reversal of paxillin phosphorylation demonstrated similar timing and adhesion-independence. Progression out of mitosis was confirmed by a decrease in cyclin B1 levels between 40 and 80 min. The actopaxin- and paxillin-binding partner, ILK, did not display changes in electrophoretic mobility in these experiments (Figure 7A).

The first two N-terminal SP sites are essential for the mitotic electrophoretic mobility shift of actopaxin *in vivo*

Finally, having demonstrated the phosphorylation of actopaxin by cyclin B1/cdc2 both *in vitro* and *in vivo*, we have performed an initial analysis to identify the target SP site(s) responsible for the mitotic mobility shift of actopaxin *in vivo*. HeLa cells were transfected with Xpress-tagged constructs of actopaxin possessing mutations in the N-terminal cdc2 kinase phosphorylation sites. Transfected cells were arrested in mitosis with nocodazole and lysates were immunoblotted with Xpress monoclonal antibody. Wild-type Xpress-tagged actopaxin exhibited a mitotic shift when compared with the asynchronous control (Figure 8, lanes 1 and 2). Mutation of Ser-14 and Ser-19 to glycine (SP sites three and four) had no effect on the mitotic shift of exogenous actopaxin (Figure 8, lanes 5 and 6). In striking contrast, when Ser-4 and Ser-8 were mutated to glycine the mobility shift of actopaxin was completely abrogated, implicating the first two SP sites of actopaxin as the target residues for phosphorylation by cyclin B1/cdc2 *in vivo* (Figure 8, lanes 3 and 4). Co-migration of phosphorylated endogenous actopaxin, and non-phosphorylated epitope-tagged actopaxin, complicated direct assessment of endogenous actopaxin in transfected cells (Figure 8, middle panel, lanes 1 and 2). However, as seen in the non-transfected mitotic HeLa cells, there was a reduction in the amount of the lower-molecular-mass form of actopaxin when compared with the asynchronous cells (Figure 8, middle panel, lanes 9 and 10). This reduction in abundance was accounted for by the actopaxin exhibiting reduced electrophoretic mobility (Figure 8, lane 10). A similar reduction in the lower-molecular-mass form of actopaxin was observed in all transfected cells analysed, indicating that introduction of exogenous actopaxin mutants did not have an effect on the phosphorylation of endogenous actopaxin (Figure 8, lanes 1–8). In addition, paxillin phosphorylation was unaffected by introduction of exogenous actopaxin constructs (Figure 8, bottom panel).

DISCUSSION

Actopaxin has previously been identified as an actin- and paxillin-binding protein that localizes to focal adhesions and is present at the leading edge of migrating cells [17]. Actopaxin and its homologues, CH-ILKBP and affixin, have been implicated in the regulation of cell adhesion and cytoskeleton reorganization during cell spreading [17,20,21]. Mutations in the paxillin-binding motif of actopaxin, or deletion of its N-terminus, result in loss of focal-adhesion localization and a reduction in cell adhesion [17]. The suggested role for actopaxin in regulating cell adhesion, coupled with the presence of consensus cdc2 sites, raises the possibility that actopaxin may play a role in the dramatic cytoskeletal reorganization and attenuation of cell adhesion observed during mitosis and cell division. In the present study we show that actopaxin is indeed phosphorylated during mitosis by cyclin B1/cdc2 kinase. *In vitro* kinase experiments showed that cdc2 kinase phosphorylated actopaxin on serine,

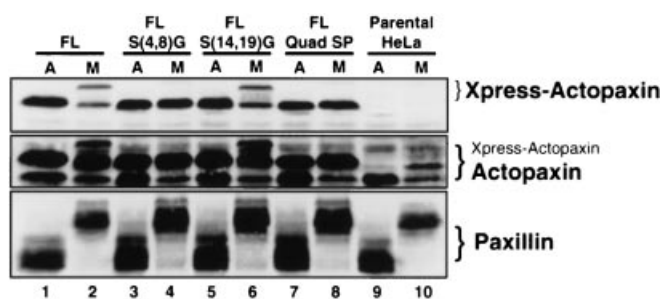


Figure 8 The first two N-terminal SP sites are essential and sufficient for the mitotically induced mobility shift of actopaxin

Western-blot analysis of whole-cell lysates from HeLa cells transfected with Xpress-actopaxin (FL), Xpress-actopaxin S(4,8)G double point mutant [FL S(4,8)G], Xpress-actopaxin S(14,19)G double point mutant [FL S(14,19)G] and Xpress-actopaxin S(4,8,14,19)G quadruple point mutant [FL Quad SP] (50 μ g total protein). In addition, non-transfected parental HeLa lysates were analysed. A and M are defined in the Figure 5 legend. The blot was probed with anti-Xpress monoclonal antibody (top panel), anti-actopaxin polyclonal antiserum (middle panel) and anti-paxillin monoclonal antibody (bottom panel). Mutating SP sites Ser-4 and Ser-8 caused the loss of the mitotic shift of Xpress-actopaxin.

and subsequent mutagenesis studies implicated the first four cdc2 sites, Ser-4, -8, -14 and -19 (Figures 2 and 3). Additionally, GST pull-down studies revealed that the N-terminus of actopaxin is able to precipitate cdc2 kinase activity (Figure 4).

To evaluate the physiological relevance of the phosphorylation detected *in vitro*, we studied the electrophoretic behaviour of actopaxin in asynchronous and mitotic lysates. Actopaxin exhibited a reduced electrophoretic mobility, specifically in mitosis (Figure 5). 2D IEF/SDS/PAGE analysis combined with alkaline phosphatase treatment provided clear evidence that this mobility shift was caused by phosphorylation (Figure 6).

To delineate the role of the N-terminal cdc2 consensus sites in the mitotic phosphorylation, we performed transfection/arrest experiments using epitope-tagged actopaxin (Figure 8). These studies showed that serine residues in the first two cdc2 consensus sites, Ser-4 and -8, are essential for the electrophoretic mobility shift observed during mitosis. However, this does not rule out phosphorylation at Ser-14 and -19. These sites may be phosphorylated and not induce an electrophoretic mobility shift and/or may require prior phosphorylation of Ser-4 and/or Ser-8. Similar co-operative phosphorylation was observed for the G subunit of protein phosphatase 1, where pre-phosphorylation of one serine residue was necessary for the protein kinase factor A/glycogen synthase kinase-3 to phosphorylate a second serine residue four amino acids away [31].

In addition to actopaxin, a number of focal adhesion and cytoskeletal proteins are known to be phosphorylated during mitosis, including paxillin, FAK, p130^{CAS}, zyxin and caldesmon ([14–16,32,33]; and K. A. West and C. E. Turner, unpublished work). The functional significance of these phosphorylation events is currently being investigated. For instance, the phosphorylation of FAK on serine during mitosis modulates its interaction with the adapter protein p130^{CAS}, which may attenuate signalling pathways mediated by these proteins [15,32]. The mitotic kinase cdc2 is known to play a pivotal role in regulating many cellular events taking place during mitosis, such as nuclear-envelope breakdown and Golgi fragmentation [34,35]. Moreover, a number of cytoskeletal proteins are phosphorylated by cdc2 kinase during mitosis, resulting in modulation of their binding activities. The phosphorylation of caldesmon by cdc2 results in

its dissociation from microfilaments and introduction of caldesmon lacking cdc2 phosphorylation sites delays entry into mitosis and inhibits cytokinesis [29,36,37]. cdc2 kinase has also been suggested to be responsible for the phosphorylation event required to promote the interaction of zyxin with the tumour-suppressor protein h-warts/LATS1 (large tumour suppressor 1) [16]. This interaction is required for targeting zyxin to the mitotic apparatus, which is crucial in controlling mitotic progression [16]. As in these instances, phosphorylation of actopaxin by cdc2 may modulate its interaction with its known binding partners: actin, paxillin and ILK. Similarly, paxillin phosphorylation may also regulate its interactions with these proteins as well as other paxillin-/actin-binding proteins, such as vinculin [38,39]. Although the cdc2 phosphorylation sites are not found within the defined binding regions for these proteins, it is reasonable to speculate that phosphorylation could cause structural changes that affect protein-binding sites proximal to the phosphorylation sites. For instance, the myristolated alanine-rich protein kinase C substrate (MARCKS) protein is phosphorylated by protein kinase C, reducing its ability to bind F-actin [40]. The reduction in F-actin binding is probably due to phosphorylation promoting a compaction of the MARCKS structure, which results in the masking of one of the actin-binding sites [41]. Alternatively, phosphorylation by cdc2 kinase may affect an as-yet-unknown interaction with actopaxin. Several families of proteins have been shown to associate with phosphoserine or phosphothreonine residues [42]. For instance, the WW domain of Pin1 has been shown to associate with the phosphoserine/proline motifs in cdc25, Plk1 and cdc27 [43]. Further study will be required to address the functional consequence of phosphorylating the SP sites in actopaxin.

It is intriguing to speculate that mitosis-dependent phosphorylation of actopaxin and paxillin may play a role in co-ordinating the disassembly of focal adhesions at the onset of mitosis. Dephosphorylation of actopaxin and paxillin coincides with progression out of mitosis and is independent of cell adhesion (Figure 7). As cells proceed out of mitosis and into G₁, they re-establish contact with the ECM and spread [4,6]. Adhesion-independent dephosphorylation suggests that dephosphorylation of actopaxin and paxillin precedes the establishment of post-mitotic cell-ECM adhesion. Further study will be required to determine whether phosphorylation of actopaxin and paxillin is necessary for focal-adhesion disassembly and if dephosphorylation of actopaxin is important in re-establishment of cell-ECM contacts.

Actopaxin belongs to a family of actin-binding proteins that includes α -parvin/CH-ILKBP (actopaxin homologues), β -parvin/affixin, γ -parvin and CLINT ([17,20,21,44]; Entrez accession no. AAL08219). α -, β - and γ -parvin show differential expression in various adult organs and during development, implying potential functional differences [44,45]. Alignment of the N-termini (Figure 1B) shows that β -parvin, γ -parvin and CLINT lack the cdc2 phosphorylation sites corresponding to Ser-4 and -8, which have been shown to be involved in the mitotic phosphorylation of actopaxin (Figure 8). In addition, β -parvin lacks the Ser-61 site observed in actopaxin, whereas CLINT possesses this site, and both proteins possess a unique putative cdc2 kinase phosphorylation site at Ser-58 (according to actopaxin numbering). The putative cdc2 phosphorylation sites found in actopaxin are absent in γ -parvin; however, a unique putative cdc2 kinase phosphorylation site is present at Ser-38. Currently, both actopaxin and β -parvin have been shown to localize to focal adhesions [17,20,21,44], whereas the subcellular localization of γ -parvin is unknown. It is intriguing to speculate that differential phosphorylation of the actopaxin/parvin family members,

possibly combined with differential localization and/or novel binding partners, is indicative of unique roles for each protein in mediating actin-cytoskeleton dynamics, not only during cell division but also in the context of cell adhesion and cell motility.

We thank Dr Kip West, Dr Michael Brown and Dr Dave Terfera for helpful comments and discussions, and Mr Brian Bouverat for expert technical assistance. This work was supported by National Institutes of Health grant GM 47607 (to C. E. T.) and a Grant-in-Aid from the American Heart Association (to C. E. T.).

REFERENCES

- Schwartz, M. A., Schaller, M. D. and Ginsberg, M. H. (1995) Integrins: emerging paradigms of signal transduction. *Annu. Rev. Cell Dev. Biol.* **11**, 549–599
- Critchley, D. R. (2000) Focal adhesions – the cytoskeletal connection. *Curr. Opin. Cell Biol.* **12**, 133–139
- Burridge, K. and Chrzanowska-Wodnicka, M. (1996) Focal adhesions, contractility, and signaling. *Annu. Rev. Cell Dev. Biol.* **12**, 463–518
- Hulleman, E. and Boonstra, J. (2001) Regulation of G1 phase progression by growth factors and the extracellular matrix. *Cell. Mol. Life Sci.* **58**, 80–93
- Assoian, R. K. and Schwartz, M. A. (2001) Coordinate signaling by integrins and receptor tyrosine kinases in the regulation of G1 phase cell-cycle progression. *Curr. Opin. Genet. Dev.* **11**, 48–53
- Assoian, R. K. (1997) Anchorage-dependent cell cycle progression. *J. Cell Biol.* **136**, 1–4
- Pines, J. (1999) Four-dimensional control of the cell cycle. *Nat. Cell Biol.* **1**, E73–E79
- Morgan, D. O. (1997) Cyclin-dependent kinases: engines, clocks, and microprocessors. *Annu. Rev. Cell Dev. Biol.* **13**, 261–291
- Jackman, M. R. and Pines, J. N. (1997) Cyclins and the G2/M transition. *Cancer Surv.* **29**, 47–73
- Davie, J. R. and Spencer, V. A. (1999) Control of histone modifications. *J. Cell. Biochem.* **32–33** (Suppl.), 141–148
- Lees, J. A., Buchkovich, K. J., Marshak, D. R., Anderson, C. W. and Harlow, E. (1991) The retinoblastoma protein is phosphorylated on multiple sites by human cdc2. *EMBO J.* **10**, 4279–4290
- Hollingsworth, Jr, R. E., Hensey, C. E. and Lee, W. H. (1993) Retinoblastoma protein and the cell cycle. *Curr. Opin. Genet. Dev.* **3**, 55–62
- Goldman, R. D., Chou, Y. H., Prahlad, V. and Yoon, M. (1999) Intermediate filaments: dynamic processes regulating their assembly, motility, and interactions with other cytoskeletal systems. *FASEB J.* **13** (Suppl. 2), S261–S265
- Yamaguchi, R., Mazaki, Y., Hirota, K., Hashimoto, S. and Sabe, H. (1997) Mitosis specific serine phosphorylation and downregulation of one of the focal adhesion protein, paxillin. *Oncogene* **15**, 1753–1761
- Yamakita, Y., Totsukawa, G., Yamashiro, S., Fry, D., Zhang, X., Hanks, S. K. and Matsumura, F. (1999) Dissociation of FAK/p130(CAS)/c-Src complex during mitosis: role of mitosis-specific serine phosphorylation of FAK. *J. Cell Biol.* **144**, 315–324
- Hirota, T., Morisaki, T., Nishiyama, Y., Marumoto, T., Tada, K., Hara, T., Masuko, N., Inagaki, M., Hatakeyama, K. and Saya, H. (2000) Zyxin, a regulator of actin filament assembly, targets the mitotic apparatus by interacting with h-warts/LATS1 tumor suppressor. *J. Cell Biol.* **149**, 1073–1086
- Nikolopoulos, S. N. and Turner, C. E. (2000) Actopaxin: a new focal adhesion protein that binds paxillin LD motifs and actin and regulates cell adhesion. *J. Cell Biol.* **151**, 1435–1448
- Dedhar, S., Williams, B. and Hannigan, G. (1999) Integrin-linked kinase (ILK): a regulator of integrin and growth-factor signalling. *Trends Cell Biol.* **9**, 319–323
- Nikolopoulos, S. N. and Turner, C. E. (2002) Molecular dissection of actopaxin-integrin-linked kinase-paxillin interactions and their role in subcellular localization. *J. Biol. Chem.* **277**, 1568–1575
- Tu, Y., Huang, Y., Zhang, Y., Hua, Y. and Wu, C. (2001) A new focal adhesion protein that interacts with integrin-linked kinase and regulates cell adhesion and spreading. *J. Cell Biol.* **153**, 585–598
- Yamaji, S., Suzuki, A., Sugiyama, Y., Koide, Y., Yoshida, M., Kanamori, H., Mohri, H., Ohno, S. and Ishigatsubo, Y. (2001) A novel integrin-linked kinase-binding protein, affixin, is involved in the early stage of cell-substrate interaction. *J. Cell Biol.* **153**, 1251–1264
- Banuelos, S., Saraste, M. and Carugo, K. D. (1998) Structural comparisons of calponin homology domains: implications for actin binding. *Structure (London)* **6**, 1419–1431
- Brown, M. C., Curtis, M. S. and Turner, C. E. (1998) Paxillin LD motifs may define a new family of protein recognition domains. *Nat. Struct. Biol.* **5**, 677–678
- Moreno, S. and Nurse, P. (1990) Substrates for p34cdc2: *in vivo* veritas? *Cell (Cambridge, Mass.)* **61**, 549–551
- Pearson, R. B. and Kemp, B. E. (1991) Protein kinase phosphorylation site sequences and consensus specificity motifs: tabulations. *Methods Enzymol.* **200**, 62–81
- Brown, M. C., Perrotta, J. A. and Turner, C. E. (1996) Identification of LIM3 as the principal determinant of paxillin focal adhesion localization and characterization of a novel motif on paxillin directing vinculin and focal adhesion kinase binding. *J. Cell Biol.* **135**, 1109–1123
- van der Geer, P. and Hunter, T. (1994) Phosphopeptide mapping and phosphoamino acid analysis by electrophoresis and chromatography on thin-layer cellulose plates. *Electrophoresis* **15**, 544–554
- Garrison, J. C. and Wagner, J. D. (1982) Glucagon and the Ca²⁺-linked hormones angiotensin II, norepinephrine, and vasopressin stimulate the phosphorylation of distinct substrates in intact hepatocytes. *J. Biol. Chem.* **257**, 13135–13143
- Yamashiro, S., Chern, H., Yamakita, Y. and Matsumura, F. (2001) Mutant caldesmon lacking cdc2 phosphorylation sites delays M-phase entry and inhibits cytokinesis. *Mol. Biol. Cell* **12**, 239–250
- Steinberg, R. A. and Coffino, P. (1979) Two-dimensional gel analysis of cyclic AMP effects in cultured S49 mouse lymphoma cells: protein modifications, inductions and repressions. *Cell (Cambridge, Mass.)* **18**, 719–733
- Dent, P. (1989) Multisite phosphorylation of the glycogen-binding subunit of protein phosphatase-1G by cyclic AMP-dependent protein kinase and glycogen synthase kinase-3. *FEBS Lett.* **248**, 67–72
- Ma, A., Richardson, A., Schaefer, E. M. and Parsons, J. T. (2001) Serine phosphorylation of focal adhesion kinase in interphase and mitosis: a possible role in modulating binding to p130(Cas). *Mol. Biol. Cell* **12**, 1–12
- Yamashiro, S., Yamakita, Y., Hosoya, H. and Matsumura, F. (1991) Phosphorylation of non-muscle caldesmon by p34cdc2 kinase during mitosis. *Nature (London)* **349**, 169–172
- Nigg, E. A., Blangy, A. and Lane, H. A. (1996) Dynamic changes in nuclear architecture during mitosis: on the role of protein phosphorylation in spindle assembly and chromosome segregation. *Exp. Cell Res.* **229**, 174–180
- Kishimoto, T. (1994) Cell reproduction: induction of M-phase events by cyclin-dependent cdc2 kinase. *Int. J. Dev. Biol.* **38**, 185–191
- Yamashiro, S., Yamakita, Y., Ishikawa, R. and Matsumura, F. (1990) Mitosis-specific phosphorylation causes 83K non-muscle caldesmon to dissociate from microfilaments. *Nature (London)* **344**, 675–678
- Hosoya, N., Hosoya, H., Yamashiro, S., Mohri, H. and Matsumura, F. (1993) Localization of caldesmon and its dephosphorylation during cell division. *J. Cell Biol.* **121**, 1075–1082
- Turner, C. E., Glenney, Jr, J. R. and Burridge, K. (1990) Paxillin: a new vinculin-binding protein present in focal adhesions. *J. Cell Biol.* **111**, 1059–1068
- Wood, C. K., Turner, C. E., Jackson, P. and Critchley, D. R. (1994) Characterisation of the paxillin-binding site and the C-terminal focal adhesion targeting sequence in vinculin. *J. Cell Sci.* **107**, 709–717
- Hartwig, J. H., Thelen, M., Rosen, A., Janmey, P. A., Nairn, A. C. and Aderem, A. (1992) MARCKS is an actin filament crosslinking protein regulated by protein kinase C and calcium-calmodulin. *Nature (London)* **356**, 618–622
- Bubb, M. R., Lenox, R. H. and Edison, A. S. (1999) Phosphorylation-dependent conformational changes induce a switch in the actin-binding function of MARCKS. *J. Biol. Chem.* **274**, 36472–36478
- Yaffe, M. B. and Elia, A. E. (2001) Phosphoserine/threonine-binding domains. *Curr. Opin. Cell Biol.* **13**, 131–138
- Lu, P. J., Zhou, X. Z., Shen, M. and Lu, K. P. (1999) Function of WW domains as phosphoserine- or phosphothreonine-binding modules. *Science (Washington, D.C.)* **283**, 1325–1328
- Olski, T. M., Noegel, A. A. and Korenbaum, E. (2001) Parvin, a 42 kDa focal adhesion protein, related to the alpha-actinin superfamily. *J. Cell Sci.* **114**, 525–538
- Korenbaum, E., Olski, T. M. and Noegel, A. A. (2001) Genomic organization and expression profile of the parvin family of focal adhesion proteins in mice and humans. *Gene* **279**, 69–79
- Thompson, T. D., Higgins, D. G. and Gibson, T. J. (1994) CLUSTAL W: improving the sensitivity of progressive multiple sequence alignment through sequence weighting, position-specific gap penalties and weight matrix choice. *Nucleic Acids Res.* **22**, 4673–4680

Received 23 October 2001/12 December 2001; accepted 31 January 2002